46th Annual Review of Progress
in Quantitative Nondestructive Evaluation
QNDE2019
July 14-19, 2019, Portland, OR, USA

QNDE2019-1234

AN ULTRASONIC FREQUENCY DOMAIN IMAGING ALGORITHM USING VIRTUAL SOURCES

Ewan Hoyle, Peter Charlton, John Rees
University of Wales Trinity Saint David
Swansea, UK

Ewan Hoyle, Mark Sutcliffe
TWI ltd
Port Talbot, UK

ABSTRACT

In this paper a frequency domain implementation of the Virtual Source Aperture (VSA) ultrasonic array imaging technique is presented. Multiple elements are fired with a phased array like delay law in order to generate a beamform as if it had originated from a virtual source located behind the aperture. Each element individually receives. The time domain Total Focusing Method (TFM) and the frequency domain phase migration methods are used to image a series of reflectors and the performance of the two imaging algorithms are measured by mapping the response of a generic reflector over a range of positions and comparing the indication intensity of the two algorithms.

Keywords: Virtual Source Aperture, Ultrasonics, Non Destructive Testing, Fourier Beamforming

1. INTRODUCTION

The TFM is a post processing method was introduced to generate fully focused images of a test specimen interior [1]. Originally, the data from the Full Matrix Capture (FMC) of an ultrasonic array was used with the TFM to generate what is is often referred to as the 'gold standard' imaging method in NDT [2]. However, the large amounts of data that is required to capture and process has been a significant factor in restraining the wide adoption of the technique [3].

VSA was developed in order to reduce the amount of data that was required to form an image of the same standard as FMC but using fewer array transmissions [4]. Instead of firing individual elements, groups of element were fired with a phased array like delay law in order to generate a wave-front as if it had originated from a virtual point behind the aperture. As more energy is used to insonify the test specimen, the returned echoes have a higher signal to noise ratio than FMC, and so a TFM image can be formed using fewer firings.

The frequency domain algorithm originated from sonar and radar, where a single source was used to transmit and receive signals [5]. This algorithm was adapted to use with ultrasonic arrays in NDT [6].Hunter *et al* [7] adapted the algorithm such that the transmitter and receiver could be at separate positions using a coordinate change known as Stolt mapping [8], originating from Geophysics. This allowed FMC imaging in the frequency domain to be achieved. The frequency domain algorithm makes efficient use of fast Fourier transforms which can allow for image forming through post processing [7]. Frequency domain imaging using virtual sources was later developed in [8].

In this paper, we investigate the time and frequency domain imaging methods using a series of reflectors and comparing the images generated by the two.

2. MATERIALS AND METHODS

2.1 Virtual Source Generation.

A virtual source can be generated using a delay law applied to multiple elements of an ultrasonic array. This is depicted in Figure 1.

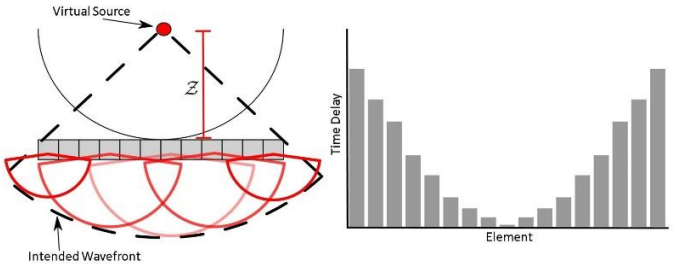

FIGURE 1: GENERATING A VIRTUAL SOURCE.

The delay applied to an element of index i in order to generate a virtual source is given by:

$$t_i = \frac{\sqrt{(i - i_0)p + z_v} - z_v}{c}$$

Here, t_i is the the delay applied to an element of index i, i_0 is the index of the center element, p is the element

pitch, z_v is the perpendicular distance of the source behind the aperture and c is the velocity of the medium.

2.2 TFM imaging (time domain)

The TFM imaging algorithm is a delay and sum approach [1] given by:

$$\sigma(x,z) = \int_0^{X_u}\int_0^{X_v} E(t(u,v),u,v)dudv$$

Where:

$$t(u,v) = \frac{\sqrt{\left(x-(u+u_0)\right)^2+(z+z_v)^2}+\sqrt{(x-v)^2+z^2}-z_v}{c}$$

Here, $\sigma(x,z)$ is the intensity value of the image at the position (x,z), $E(t,u,v)$ is the amplitude of the signal at time t for a a virtual source at position u and receiver at v. This is depicted in Figure 2. $X_u$is the horizontal distance between the first and the last virtual source and X_v is the distance between the first and the last receiving element.

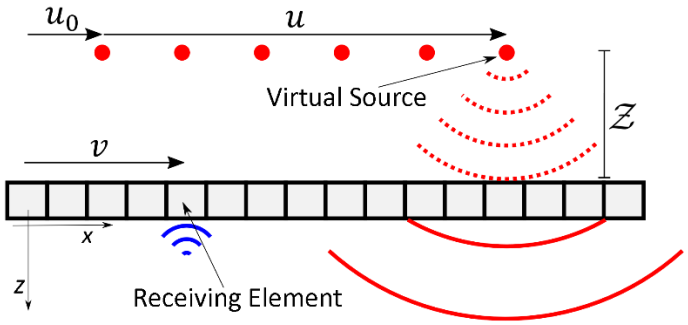

FIGURE 2: DEPICTING THE ARRAY SETUP.

2.3 Frequency Domain imaging

The frequency domain algorithm is derived for FMC in [7] and virtual sources in [9]. The summary of the implementation is seen here:

1. 3 dimensional Fourier Transform on the collected data: $E(t,u,v) \rightarrow E'(k,k_u,k_v)$ where k is the spatial frequency in the propagation direction and k_u and k_v are the spatial frequencies in the horizontal direction regarding the transmit and receive coordinates.
2. Frequency shift to account for the scan start gate and virtual source positions:
   $$E(k,k_u,k_v) = E'(k,k_u,k_v)e^{ik_uu_0+\frac{ikt_0}{c}-iz_v\sqrt{k^2-k_u^2}}$$
   Here, t_0 is the start gate of the scan.
3. Coordinate change known as Stolt mapping [8] to get the data from the transducer domain to the image domain. This is done by keeping k_u constant: $E(k,k_u,k_v) \rightarrow E(k_x,k_z|k_u)$ and using a linear interpolation function.
4. Sum over all k_u values: $E(k_x,k_z) = \int_{-\infty}^{\infty} E(k_x,k\_z|k_u)\,dk_u$
5. Inverse 2 dimensional Fourier transform to obtain the image $E(k_x,k_z) \rightarrow E(x,z)$

The coordinate change uses equations:

$$k_v = k_x - k_u$$

And

$$k = \pm\frac{\sqrt{k_z^4+2(k_u^2+(k_x-k_u)^2)k_z^2+k_u^4+(k_x-k_u)^4-2(k_x-k_u)^2k_u^2}}{2k_z}$$

The spatial frequencies k_x and k_z are real and satisfy the equation:

$$k = \sqrt{k_x^2+k_z^2}$$

3. RESULTS AND DISCUSSION

An array of 64 elements with a pitch of 0.6mm was simulated using the CIVA software. Each element had a center frequency of 5MHz. 25 virtual sources were used, each at the center of a smaller sub-aperture that was incremented along the array. The sub aperture consisted of 16 elements and was incremented by 2 elements between each transmission. The distance of the virtual source behind the aperture was 5mm.

The time domain signal recorded 4098 sample points for each transmit/receive pair, at a sampling frequency: f_s = 50MHz, with the first recording at when the first element was fired. The transmit and receive points were discretely sampled with a spacing of p_u and p_v. Therefore the spatial frequency components obtained from the initial 3D Fourier transform were ranging from: $k_u = -\frac{1}{2p_u} \rightarrow \frac{1}{2p_u}$, $k_v = -\frac{1}{2p_v} \rightarrow \frac{1}{2p_v}$ and $k = -\frac{f_s}{2c} \rightarrow \frac{f_s}{2c}$.). The data was padded with zeros such that the data in the k_u and k_v directions was double their original size. The spatial frequency components in the horizontal and vertical direction were respectively: $k_x = -\frac{1}{2p_x} \rightarrow \frac{1}{2p_x}$ and $k_z = -\frac{1}{2p_z} \rightarrow \frac{1}{2p_z}$, where p_x and p_z was the spacing of the image pixels in the horizontal and vertical direction (both 0.2mm).

A series of side drilled holes was simulated, each with a diameter of 1mm and were spaced in a square lattice 4mm apart in a steel test specimen with a longitudinal velocity of 5900 ms^{-1}. The data was simulated using the CIVA software, with artificial noise added in. Each hole was simulated and processed separately to avoid interfering signals. The images of all the side drilled holes were then combined in one image by displaying the maximum intensity of each pixel. Each image is normalized to the response of a side drilled located at 16mm depth and 2mm from the center axis.

The images of the side drilled holes from the time and frequency domain algorithms can be seen in Figures 3 and 4 respectively. It was found that the signal to noise ratio of the frequency domain algorithm was 6dB higher compared to that of the time domain. Therefore, 6dB of soft gain has been added into the frequency domain image for a fair comparison. The actual

location of the side drilled holes are displayed as blue circles overlaying the image for reference.

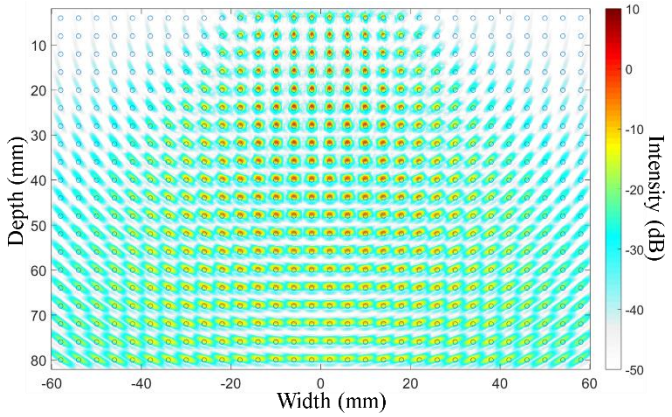

FIGURE 3: TIME DOMAIN ALGORITHM SDH IMAGE

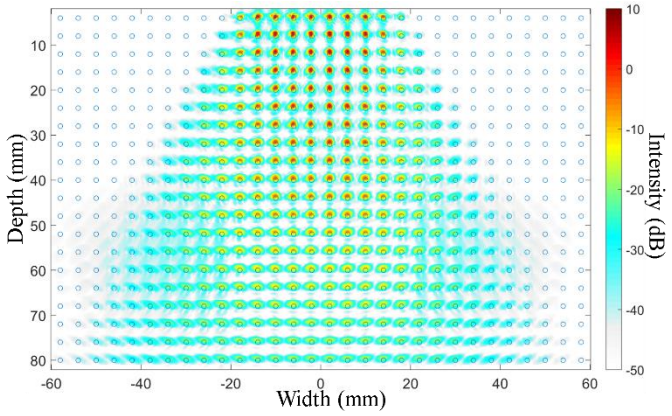

FIGURE 4: FREQUENCY DOMAIN ALGORITHM SDH IMAGE

Although the signal to noise ratio of the side drilled hole indication calibrated against was higher for the frequency domain than that of the time domain, it can be seen that the time domain algorithm provides a wider field of view than the frequency domain. The intensity of the indications from holes further away from the transducer and also at higher steering angles are comparatively higher. Therefore, the time domain algorithm is likely to be the more useful algorithm in general, unless a short-range inspection in a noisy material is performed.

Sampling a larger number of frequency components during the coordinate transform may help to improve the image. It could also be useful to use filtering to remove frequency components that only contribute noise to certain pixels, as this may help to improve the image contrast. Further work is required in order to investigate this and find the optimum implementation of the frequency domain algorithm.

4. CONCLUSION

The study indicates that the time domain algorithm gives a wider field of view and a higher intensity value for deeper indications when compared to the frequency domain. The signal to noise ratio of the indications from the frequency algorithm is higher closer to the transducer, making it ideal for short range inspections in noisy materials. However, the indications from the frequency domain algorithm attenuate quicker for a larger distance and a wider range of angles when compared to the time domain. Further work is required in order to confidently conclude these findings, as the implementation of the frequency domain algorithm could be improved with further investigation.

ACKNOWLEDGEMENTS

The work was funded by the European Social Fund through the KESS 2 scholarship scheme at the University of Wales Trinity Saint David, and supported by TWI ltd.

REFERENCES

[1] C. Holmes, B. W. Drinkwater, and P. D. Wilcox. Post-processing of the full matrix of ultrasonic transmit-receive array data for non-destructive evaluation. NDT&E International, 38:701–711, 2005.

[2] J. F. Cruza, J. Camacho, and C. Fritsch. Plane-wave phase-coherence imaging for NDE. NDT&E International, 87(September 2016):31–37, 2017.

[3] M. Sutcliffe, M. Weston, B. Dutton, P. Charlton, and K. Donne. Real-time full matrix capture for ultrasonic non-destructive testing with acceleration of post-processing through graphic hardware. NDT&E International, 51:16–23, 2012.

[4] M. Sutcliffe, P. Charlton, and M. Weston. Multiple virtual source aperture imaging for non-destructive testing. Insight: Non-Destructive Testing and Condition Monitoring, 56(2):75–81, 2014.

[5] P. Gough and D. Hawkins. Unified Framework for Modern Synthetic Aperture Imaging Algorithms. John Wiley & Sons Imaging Systems Technology, 8:343–358, 1997.

[6] T. Stepinski. An Implementation of Synthetic Aperture Focusing Technique in Frequency Domain. IEEE Transactions on Ultrasonics, Ferroelectrics, and Frequency Control, 54(7), 2007.

[7] A. J. Hunter, B.W. Drinkwater, and P. D.Wilcox. TheWavenumber Algorithm for Full-Matrix Imaging Using an Ultrasonic Array. IEEE Transactions on Ultrasonics, Ferroelectrics and Frequency Control, 55(11):2450–2462, 2008.

[8] R. H. Stolt. Migration by Fourier Transform. Geophysics, 43(1):23–48, 1978.

[9] Synthetic Aperture Ultrasound Fourier Beamformation Using Virtual Sources IEEE transactions on ultrasonics, ferroelectrics and frequency control, 63(11)